

Cored Rutherford Cables for the GSI Fast Ramping Synchrotron

M.N. Wilson, A.K. Ghosh, B. ten Haken, W.V. Hassenzahl, J. Kaugerts, G. Moritz, C. Muehle, A. den Ouden, R. Soika, P. Wanderer, W. A. J. Wessel.

Abstract—The new heavy ion synchrotron facility proposed by GSI will have two superconducting magnet rings in the same tunnel, with rigidities of 200T·m and 100T·m. Fast ramp times are needed, which can cause significant problems for the magnets, particularly in the areas of ac loss and field distortion. This paper discusses the 200T·m ring, which will use $\text{Cos}\theta$ magnets based on the RHIC dipole design. We discuss the reasons for choosing Rutherford cable with a resistive core and report loss measurements carried out on cable samples. These measurements are compared with theoretical calculations using measured values of inter-strand resistance. Reasonably good agreement is found, but there are indications of non-uniformity in the adjacent resistance R_a . Using these measured parameters, losses and temperature rise are calculated for a RHIC dipole in the operating cycle of the accelerator. A novel insulation scheme designed to promote efficient cooling is described.

Index Terms— ac loss, dipole magnet, field error, superconducting synchrotron, Rutherford cable.

I. INTRODUCTION

GSI is planning a new heavy ion accelerator consisting of two superconducting synchrotron rings placed one above the other in the same tunnel [1], and ramping with a rise time of a few seconds. The lower ring, having a magnetic rigidity of 100T·m, will use magnets based on the Nuclotron design [2] and the upper 200T·m ring will use magnets based on the RHIC design [3]. Here we consider the cable for the RHIC dipoles, which use a single layer $\text{Cos}\theta$ winding. To reach the high average intensities required by the project, it will be necessary to ramp the magnets at a rate of $\sim 1\text{T/s}$, with the following operating cycle:

inject at 0.4 T
ramp up to 4T at 1T/s
extract at 4T for 5 s
ramp down at 1 T/s

To date, superconducting accelerators with high field magnets have all worked at relatively slow ramp rates and have been able to use Rutherford cable without incurring too much ac loss. At 1T/s however, coupling between the strands of a conventional Rutherford cable would produce high ac losses and unacceptable field distortion. Coupling may be reduced by increasing the resistance between strands in the cable, but there are reasons to believe that this can impede current sharing and thereby make the magnet more susceptible to quenching at high ramp rates. Because coupling in Rutherford cables is very anisotropic, it may be reduced greatly by increasing the crossover resistance via a core foil, while still leaving a low resistance in the other direction. Cables with core foils were first tried more than 20 years ago [4] and have been the subject ongoing research [5]. We are hopeful that cores will reduce the losses without affecting current sharing. We first discuss the general question of losses and current sharing, leading to our choice of a cored cable. Loss measurements on prototype cables are described and compared with theoretical predictions based on Ohmic measurements of inter-strand resistance. This formulation is then used to predict the loss and temperature rise in an operational dipole magnet. A novel insulation scheme with cooling holes in the Kapton wrap is described.

II. CURRENT SHARING AND LOSSES

Coupling currents in a Rutherford cable flow between the strands via two kinds of inter-strand resistance: the *crossover resistance* R_c and *adjacent resistance* R_a as sketched in Fig 1.

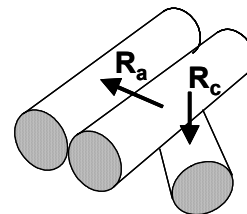


Fig. 1: Crossover and adjacent resistances between strands in a cable (note that R_a is defined to be over the same length of wire that R_c occupies).

We can reduce coupling losses by increasing R_c and R_a – so why not simply make the inter-strand resistance as large as is

Manuscript received August 5 2002. This work was supported in part by the U.S. Department of Energy under Contract No. DE-AC02-98CH10886

M. N. Wilson (corresponding author) is a consultant at Brook House, 33 Lower Radley, Abingdon, OX14 3AY, UK. (email: m-wilson@clara.co.uk).

G. Moritz, J. Kaugerts and C. Muehle are with GSI, Abteilung BTE, Planckstrasse 1, D-64291, Darmstadt, Germany. (emails: G.Moritz@gsi.de, j.kaugerts@gsi.de and C.Muehle@gsi.de)

A.K. Ghosh, R. Soika and P. Wanderer are with the Brookhaven National Laboratory, Upton NY, 11973, USA. (e-mails: aghosh@bnl.gov, soika@bnl.gov and wanderer@bnl.gov).

W.V. Hassenzahl is with Advanced Energy Analysis, 1020 Rose Avenue, Piedmont, CA 94611, USA. (e-mail: advenergy1@aol.com).

B. ten Haken, A. den Ouden and W. E. J. Wessel are with the Low Temperature Division, University of Twente, PO Box 217, 7500 AE Enschede, Netherlands (e-mails: b.tenhaken@tn.utwente.nl, A.denOuden@tn.utwente.nl and w.a.j.wessel@tn.utwente.nl).

needed to reduce losses to the required level? The main reason for not doing so is that a high inter-strand resistance seems to degrade the quench current at high ramp rates; we suggest two possible mechanisms for this. Firstly, it has been shown experimentally and theoretically [6] that partially soldered cables (low R_c and R_a) have a minimum quench energy MQE at high currents which is $\sim 5x$ higher than the same cable unsoldered (high R_c and R_a). Thus a low inter-strand resistance seems to bring greater stability against random disturbances (eg wire movement) in the magnet.

Secondly there is the phenomenon of ramp rate induced quenching, found in some fusion magnets and investigated in detail during the development of magnets for the SSC High Energy Booster [7]. As shown in Fig 2, these magnets went to their full critical current at slow ramp rates, but quenched early when the current was ramped up quickly. Two types of behavior were identified. Type A magnets showed no reduction in quench current until a rate of $\sim 25A/s$ was reached, after which the quench current decreased more or less linearly with ramp rate. Type B magnets however suffered a rapid drop in quench current at quite small ramp rates. In general, it was found that magnets with small inter-strand resistance were Type A and those with large inter-strand resistance were type B. For example the Type A magnet in Fig. 2 had $R_c = 9 \mu\Omega$ and Type B had $R_c = 80 \mu\Omega$.

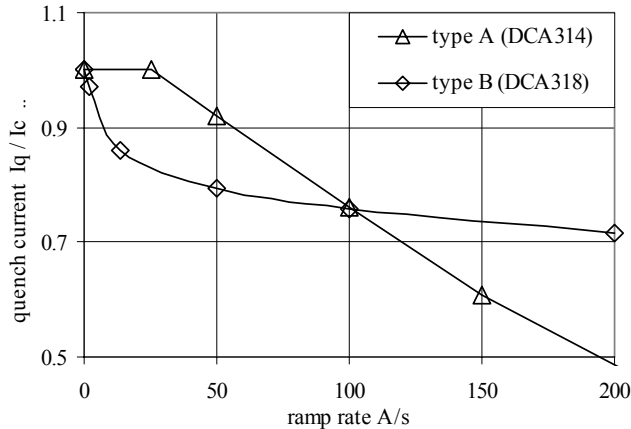


Fig. 2: Quench current of SSC magnets as a function of ramp rate [5].

A plausible explanation of this behavior is that Type A quenching is caused by heating due to the ac losses arising from strong inter-strand coupling. Type B quenching is thought to be caused by non-uniform current distribution between the strands. It is well known that the current does not divide equally between the strands in accelerator magnets, as evidenced by the periodic variation of field along the length of the magnet, which has the same periodicity as the cable twist [8]. During ramping, if one strand has more current than its neighbors, it will reach critical current early and be driven into the flux-flow resistance region. When there is a good electrical contact to neighboring strands, the flux-flow voltage will drive some current into those strands and produce a more uniform distribution. If however the electrical contact is not good, the 'victim' strand will have to go much further into the

flux flow region in order to generate sufficient voltage to transfer the current. This extra flux-flow resistance may be enough to trigger a quench.

As discussed later, we are fairly confident that our new system of cooling holes will allow us to control Type A quenching, but we are nervous about Type B quenching. In the absence of a definite theory, we have therefore decided to make the contact resistance high enough to control the losses, but no higher than necessary. To quantify how high, we need to look at the three types of inter-strand coupling in Rutherford cable.

a) Cable coupling via R_c in transverse field

$$P_{tc} = \frac{1}{120} \frac{\dot{B}_t^2}{R_c} \frac{c}{b} p N(N-1) \quad (1)$$

where P_{tc} is the coupling loss per unit volume of cable, p is the cable twist pitch, \dot{B}_t is the rate of change of field transverse to the broad face of the cable, N is the number of strands, c is the half width of the cable and b is its half thickness.

b) Cable coupling via R_a in transverse field

$$P_{ta} = \frac{1}{24} \frac{\dot{B}_t^2}{R_a} (N-1) \frac{p}{\cos^2 \theta} \quad (2)$$

where θ is the slope angle of the wire relative to the cable length ($\cos \theta \sim 1$).

c) Cable coupling via R_a in parallel field

$$P_{pa} = \frac{1}{32} \frac{\dot{B}_p^2}{R_a} (N-1) p \frac{b^2}{c^2} \frac{1}{\cos^2 \theta} \quad (3)$$

where \dot{B}_p is the rate of change of field parallel to the broad face of the cable. Because c is always much greater than b , it may be seen immediately that the loss in transverse field is much greater than in parallel field. From (1) and (2) we see that the ratio:

$$\frac{P_{tc}}{P_{ta}} = \frac{R_a}{R_c} \left\{ \frac{N}{5} \frac{c}{b} \cos^2 \theta \right\} \quad (4)$$

A typical value for the factor in brackets is ~ 50 , which means that a given crossover resistance causes 50 times more loss than the same adjacent resistance. It follows that we can make $R_a \sim R_c / 50$ without increasing the loss too much. It is this inherent anisotropy in the loss mechanism that is the reason for choosing cored cables.

III. SAMPLES AND LOSS MEASUREMENT

Figs. 3 and 4 show cross sections of our prototype cable with a 25 μm stainless steel core in its centre. In other respects it is the same as the RHIC dipole cable [3].



Fig 3: cross section of a cored cable

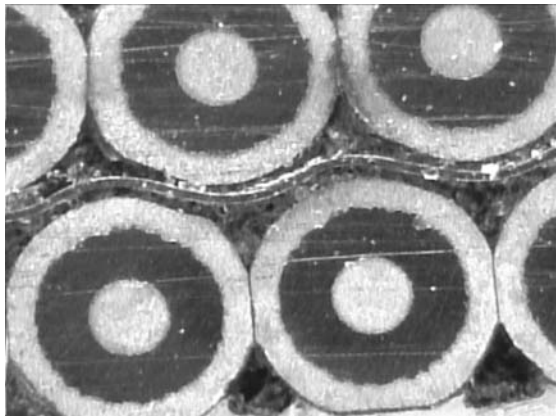


Fig. 4: local region showing the stainless steel core foil.

Table I lists the common parameters of the cables tested, very similar to the RHIC dipole cables. The wires, manufactured by Oxford Superconducting Technology, were coated with ‘Staybrite’ silver tin alloy and cabled by New England Electric.

TABLE I: COMMON PARAMETERS OF THE CABLES TESTED

cable twist pitch	p	74mm
cable mean half thickness	b	0.583mm
cable half width	c	4.93mm
wire diameter	d_w	0.648mm
wire copper / NbTi ratio	m	2.25
filament diameter	d_f	6 μ m

Cables were made with different cores; Table II lists the parameters. Our preferred core material is stainless steel, but a brass core was also tested to get a result with lower R_c . Early attempts to use an anodized titanium foil were abandoned because the foil broke up during cabling. Even the stainless steel suffered some punching through near the (narrow) inner edge of the cable. To avoid this problem, we made cable 003E with two stainless steel cores. Adding the cores increased the half thickness by 4 to 7 μ m above the value shown in Table I, so the compaction was somewhat greater than RHIC cable.

TABLE II: VARYING PARAMETERS OF THE CABLES TESTED

cable	core	wire twist pitch
003B	1 x 25 μ m stainless	4mm
003E	2 x 25 μ m stainless	6mm
003F	1 x 50 μ m brass	6mm

Losses were measured at the University of Twente. The sample, comprising 10 pieces of cable, each 375mm long, was first compressed to 60Mpa and heated to 225C in a cycle which simulates the RHIC cure cycle for the Kapton insulation. The sample was then unloaded, transferred to the measurement sample holder and re-compressed to 60Mpa. Losses were measured calorimetrically [9] in a superconducting dipole magnet, generating a sinusoidal oscillating field of $\pm 0.3T$ at frequencies up to 250mHz. By rotating the sample, the field could be oriented parallel or transverse to the face of the cable. Losses were measured in

terms of gas flow, which was calibrated over the measurement range to an accuracy of 2%. After a settling time of 10 minutes, each flow measurement was made for 5 minutes. Fig. 5 shows a typical result of loss per cycle versus frequency.

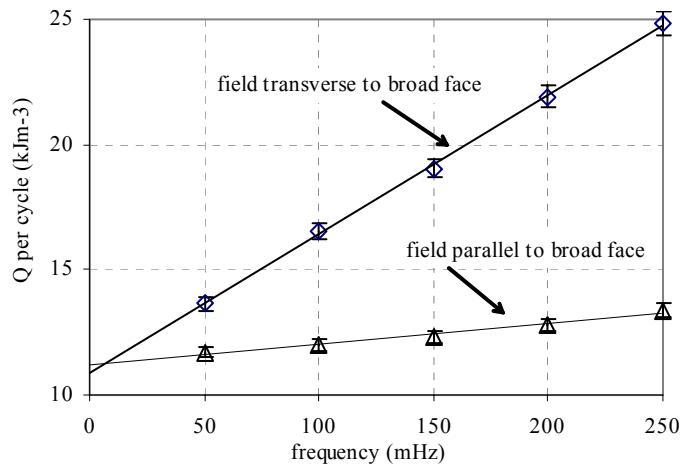


Fig. 5: Typical loss measurement on cable 003E

Previous experience has shown us that the inter-strand contact resistance can vary greatly between different cool-downs of the same sample [10]. For this reason, we made $V-I$ measurements of R_a on one length of the cable sample *in situ* during the same cool-down as the loss measurement. For cored cables however, R_c is so high as to be invisible in the usual $V-I$ measurement and must be measured separately in a cut sample [11].

In order to separate the cable coupling loss from loss within the individual wires, the magnetization of a single wire with 13mm twist pitch was measured at several different ramp rates. From this measurement we can derive the coupling and hysteresis losses in the wire.

IV. ANALYSIS OF THE LOSS MEASUREMENTS

Our objective is to derive parameters and verify a model which can be used to predict losses in the synchrotron. We therefore start by using this model to predict the losses measured at Twente and then compare the results.

We start by using the wire magnetization measurements to derive two parameters:

- J_c as a function of B , which is then used to calculate hysteresis loss.
- the effective transverse resistivity across the wire ρ_{et} which is used to calculate coupling loss within the wire.

Starting with b), we plot the wire magnetization M against dB/dt at several different fields and find a straight line, as expected from:

$$M_e = \frac{2 \dot{B} \tau_f}{\mu_o} \quad (5)$$

where τ_f is the inter-filament coupling time constant

$$\tau_f = \frac{\mu_o}{2\rho_{et}} \left\{ \frac{p}{2\pi} \right\}^2 \quad (6)$$

and ρ_{et} is the effective transverse resistivity across the wire, depending on the copper matrix, the interface resistance between NbTi and copper, and the geometry.

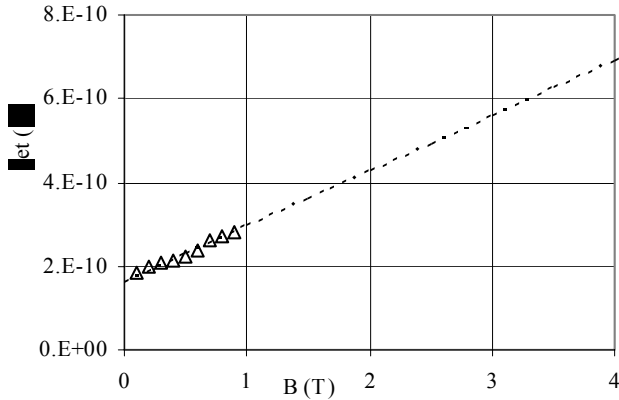


Fig. 6: Measured values of ρ_{et} for a wire of 13mm twist pitch, dashed line shows magnetoresistance of copper, scaled to fit at low field.

Fig. 6 shows a plot of our measured ρ_{et} as a function of B . Also shown for comparison is the magnetoresistance for copper [12] of similar RRR (~ 220), scaled to fit at low field and showing a remarkably good agreement in variation with field.

By extrapolating the measured magnetization back to zero \dot{B} , we obtain the persistent magnetization of individual filaments, as plotted in Fig. 7, where the four quadrants of a symmetrical $\pm B$ magnetization loop have been plotted in the all positive quadrant.

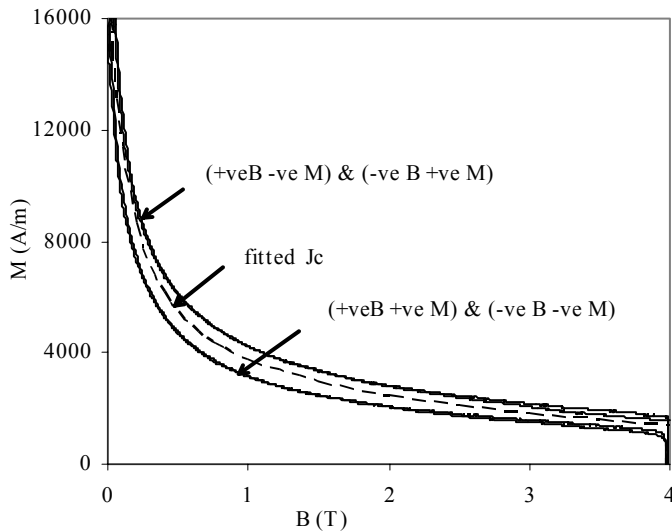


Fig. 7: Magnetization of a single wire extrapolated to zero \dot{B} and plotted in the all positive quadrant; dashed line shows fitted J_c .

The difference between 'odd' and 'even quadrants is caused partly by field profile within the filaments, but mainly by reversible magnetization of the NbTi. To a good approximation, we may take a mean between them and calculate the bulk J_c from:

$$M_f = \frac{2}{3\pi} \lambda_f J_c d_f \quad (7)$$

where λ_f is the filling factor and d_f is the filament diameter. We fit the current density with a modified Kim Anderson approximation.

$$J_c = \frac{J_o B_o}{B + B_o} + A_0 + A_1 B \quad (8)$$

For the data of fig 6, we find:

$$J_o = 4 \times 10^{10} \text{ A.m}^{-2}$$

$$B_o = 0.155 \text{ T}$$

$$A_0 = 4.8 \times 10^9 \text{ A.m}^{-2}$$

$$A_1 = -7.0 \times 10^8 \text{ A.m}^{-2}.\text{T}^{-1}$$

The methods of measuring R_c and R_a are described in [11] and these complete our list of parameters needed to calculate the losses. For a sinusoidal waveform of angular frequency ω and amplitude $\pm B_a$ we use the following formulae for loss per cycle:

a) Cable coupling via R_c in transverse field

$$Q_{tc} = \frac{\pi\omega B_a^2}{120 R_c} N(N-1) p \frac{c}{b} \quad (9)$$

b) Cable coupling via R_a in transverse field

$$Q_{ta} = \frac{\pi\omega B_a^2}{24 R_a} (N-1) \frac{p}{\text{Cos}^2\theta} \quad (10)$$

c) Cable coupling via R_a in parallel field

$$Q_{pa} = \frac{\pi\omega B_a^2}{32 R_a} (N-1) \frac{b^2}{c^2} \frac{p}{\text{Cos}^2\theta} \quad (11)$$

d) Inter filament coupling in the wires

$$Q_f = \lambda_w 2\pi \frac{B_a^2}{\mu_o} \omega \tau_f \quad (12)$$

e) Hysteresis in the filaments

$$Q_h = \frac{8}{3\pi} \lambda_w \lambda_f d_f \left\{ J_o B_o \ln \left(\frac{B_a + B_o}{B_o} \right) + A_0 B_a + A_1 \frac{B_a^2}{2} \right\} \quad (13)$$

where λ_w and λ_f are the filling factors of wire in the cable and NbTi filaments in the wire.

With these formulae and the measured ρ_{et} , J_c , R_a & R_c we calculate losses at 250mHz with a field amplitude $B_a = 0.3\text{T}$ as listed in Table III. For the filament coupling we take $\rho_{et} = 1.9 \times 10^{-10} \Omega.\text{m}$, as shown in Fig. 6, at the mean of the sinusoidal field, $B = 0.15\text{T}$. Of course, the measurements cannot distinguish between different types of coupling loss, so we also list the total calculated coupling loss for each field direction.

The $V-I$ measurements in [9] indicate that R_a varies strongly across the cable, being much lower at the edges (Table III lists the average value). A simple calculation shows that if all the R_a is located at the edge of the cable, the adjacent coupling in transverse field is increased by a factor 3. For this reason, we include a line 'total coupling transverse with edge R_a ' in Table III, where the Q_{ta} term has been increased to $3 \times Q_{ta}$.

Table IV compares the calculations with measurement.

Firstly the hysteresis, which of course should not depend on field direction. It may be seen that the results are in reasonable agreement; deviations are probably caused by differences in J_c between the cable and our measured wire. Secondly the transverse coupling, where the losses for cables B and E are nicely bracketed by the factor 3 edge enhancement in R_a . Cable F does not seem to show any edge enhancement, we don't know why.

In general however, we feel these calculations are in reasonable agreement with experiment and are good enough for outline design of the synchrotron. They do not suggest that the conventional theory is deficient or that we need to postulate additional current paths as suggested in [5].

TABLE III: CALCULATED LOSSES (J/CYCLE)

	cable	003B	003E	003F
crossover resistance	R_c	1.4E-02	6.3E-02	6.6E-04
adjacent resistance	R_a	5.0E-05	4.9E-06	4.6E-06
wire twist pitch	p_w	4.0E-03	6.0E-03	6.0E-03
transverse crossover loss	Q_{tc}	144	32	3050
transverse adjacent loss	Q_{ta}	845	8628	9282
parallel adjacent loss	Q_{pa}	9	91	98
fil't coupling time const	t_f	1.3E-03	2.9E-03	2.9E-03
filament coupling loss	Q_f	785	1767	1767
filament hysteresis	Q_h	10925	10925	10925
total coupling transverse	$Q_{tc}+Q_{ta}+Q_f$	1774	10427	14099
total coupling transverse with edge R_a	$Q_{tc}+3^*Q_{ta}+Q_f$	3464	27684	32662
total coupling parallel	$Q_{pa}+Q_f$	794	1858	1865

TABLE IV: EXPERIMENTAL LOSSES COMPARED WITH CALCULATION (J/CYCLE)

	cable	003B	003E	003F
hysteresis transverse		10230	10849	11350
hysteresis transverse exp/theo		0.94	0.99	1.04
hysteresis parallel		10073	11201	11683
hysteresis parallel exp/theo		0.92	1.03	1.07
coupling transverse		2974	13915	12460
coupling transverse exp/theo		1.68	1.33	0.88
coupling trans + edge R_a exp/theo		0.86	0.50	0.38
coupling parallel		1008	2070	1082
coupling parallel exp/theo		1.27	1.11	0.58

V. LOSSES IN THE SYNCHROTRON

We now use this data to predict losses in a dipole of the synchrotron SIS200 [1] when operating under the ramping cycle described in the introduction, using the method of calculation described in [10]. The dipole is 2.6m long and the cables are based on the samples tested, but with a reduced copper/NbTi ratio of 1.8:1 and a wire twist pitch of 4mm.

Loss power is calculated during ramping and also averaged over the whole cycle. To allow for low R_a on the cable edge, the loss Q_{ta} is multiplied by a factor which just brings the theory into line with the measurements in Table IV. Table V presents the results, starting with our lowest loss cable 003B. It may be seen that hysteresis is by far the largest component of loss. We therefore include a second column, having the 003B cable parameters, but with 3.5 μ m filaments, chosen as our estimate of the smallest diameter possible without incurring too much proximity coupling in a pure copper matrix. In fact the 003B3.5 column includes an estimate of proximity coupling, based on [13], which adds \sim 10% to the hysteresis loss.

If ramp rate quenching turns out to be a problem, it may be necessary to use a lower inter-strand resistance, so the third column is based on cable 003F. It may be seen that the lower R_a and R_c have roughly doubled the total loss.

Finally, the last column is included with the same R_a as 003B, but with $R_a = R_c$ to represent a cable with no core. It may be seen that this has increased the loss substantially. Of course, if an inter-strand resistance similar to 003F turns out to be necessary, the no-core loss would be extremely high.

TABLE V: LOSSES CALCULATED FOR THE SYNCHROTRON

	cable	003B	003B3.5	003F	002NC
crossover R_c	$\mu\Omega$	1.4E-02	1.4E-02	6.6E-04	5.0E-05
adjacent R_a	$\mu\Omega$	5.0E-05	5.0E-05	4.6E-06	5.0E-05
edge factor		2.5	2.5	1.0	1.0
filament diameter d_f	μ m	6.0E-06	3.5E-06	6.0E-06	6.0E-06
ramping power P_r	Watt	13.1	9.9	24.3	47.4
average power P_{av}	Watt	7.7	5.9	14.3	28.0
<i>loss components as a fraction of the total</i>					
transverse crossover P_{tc}		1.0%	1.3%	11.2%	75.7%
transverse adjacent P_{ta}		18.8%	24.8%	44.3%	2.1%
parallel adjacent P_{pa}		0.2%	0.3%	1.3%	0.1%
filament coupling P_f		12.4%	16.4%	6.7%	3.4%
hysteresis P_h		67.6%	57.3%	36.5%	18.7%

The losses in Table V are somewhat higher than presented in [10] because our measured ρ_{et} is lower than earlier estimates, the matrix ratio is reduced to 1.8:1 and J_c is higher.

VI. TEMPERATURE RISE AND COOLING

For good cooling during the ramp, we have developed a new insulation with cooling holes cut by laser in the Kapton wrap along the inner edge of the cable, as shown in Fig.8.

Trial sections of coil have been made from cable with this insulation and found to have an inter-turn voltage breakdown of \sim 1.5kV, giving a comfortable safety margin against the expected ramping and quench voltages in the dipole.

Cooling in the dipole will be provided by forced-flow supercritical helium along the inner surface of the winding, so the temperature rise in the cable has two components:

- conduction across the width of the cable.
- heat transfer to the helium.

Heat is conducted across the cable in two ways:

- i) via the thermal resistance between adjacent wires.
- ii) along the wires in a diagonal direction.



Fig. 8: Cooling slots cut by laser on the inner edge of the cable

We estimate i) from R_a assuming the Wiedemann-Franz Law: a reasonable guess but not, to our knowledge, verified for contact resistances. Heat transfer is estimated via a Dittus-Boelter correlation for supercritical helium [14], assuming the coolant to be at 4.4K with a pressure of 5 atm. and flow rate of 100 gm/sec. Table VI summarizes the temperature rises a) and b) plus the total, for an insulation in which the slots expose 26% of the cable inner edge. It may be seen that temperature drops across the cable are negligible and that, even with such a small cooling area, the heat transfer temperature rises are small.

With no cooling slots at all, the temperature drop across the Kapton would be $\sim 0.2K$. Much more serious however is the likely prospect of a static gas film between the Kapton and cable, in which case the temperature drop would be $\sim 1.5K$ - far too near the allowable temperature margin for any practical accelerator.

TABLE VI: CALCULATED TEMPERATURE RISES

	cable	003B	003F
$\Delta\theta$ cable	mK	9	8
$\Delta\theta$ heat transfer	mK	70	128
$\Delta\theta$ total	mK	79	136

VII. CONCLUSION

Cored Rutherford cables are the preferred choice for the proposed GSI fast pulsed synchrotron because they have reasonable losses, while retaining a low inter-strand resistance.

We have shown that the measured losses of three different cored cables can be explained reasonably well in terms of conventional theory. Because of the variability of inter-strand resistance, it is important to measure it in situ, during the same cool-down as the loss measurement. There seems to be some enhancement of loss in transverse field caused by the adjacent resistance R_a being lower at the cable edges.

Extrapolating these measured values to the planned synchrotron we find acceptable levels of loss. Using our new insulation with cooling holes, we calculate temperature rises in the cable which will not significantly degrade its performance.

There are good reasons to believe that a low inter-strand resistance in the cable will be helpful in reduce the sensitivity of quench current to high ramp rates, but this remains conjectural at present. It can only be verified by testing prototype magnets, due to start later this year.

ACKNOWLEDGEMENT

We are grateful to G. Staupendahl and colleagues at the Technical University of Jena for developing techniques for producing cooling holes in the insulation and to A. P. Verweij at CERN for help in interpreting the $V-I$ data on inter-strand resistance

REFERENCES

- [1] G. Moritz, "Superconducting Magnets for the 'International Accelerator Facility for Beams of Ions and Antiprotons' at GSI", paper 4LA01 at this conference.
- [2] A.D. Kovalenko, N.N. Agapov, A.M. Donyagin, H.G. Khodzhbagiyani, G.L. Kuznetsov, G. Moritz, G. Hess, J. Kaugerts, E. Fischer and C. Muehle, "Superferric Model Dipole Magnet with the Iron Yoke at 80K for the GSI Future Fast Cycling Synchrotron", paper 4LA02 at this conference.
- [3] M. Anerella, J. Cozzolino, J. Escallier, G. Ganetis, A. Ghosh, R. Gupta, M. Harrison, A. Jain, S. Kahn, E. Killian, W. Louie, A. Marone, J. Muratore, S. Plate, M. Rehak, W. Sampson, J. Schmalzle, R. Thomas, P. Thompson, P. Wanderer, E. Willen, "The RHIC Magnet System" to be published in Nucl. Inst. Meth. preprint available at <http://www.bnl.gov/magnets/publications/index.asp>
- [4] D. Wake, D. Gross, R. Yamada and B Blatchley, IEEE Trans MAG-15, No 1, pp141, (1979).
- [5] M. D. Sumption, E.W. Collings, R. M. Scanlan, S.W. Kim, M. Wake, T. Shintomi, A. Nijhuis and H.J. ten Kate, "AC loss in cored stabrite cables in response to external compaction and variation in core thickness and width", Cryogenics 41 (2001) 733-744.
- [6] A. K. Ghosh, W. B. Sampson and M. N. Wilson, 'Minimum Quench Energies of Rutherford cables and Single Wires', IEEE Trans Appl. Superconductivity Vol 7, No 2, pp954 (1997).
- [7] A. Devred and T. Ogitsu, "Ramp Rate Sensitivity of SSC Magnet Prototypes", pp184-308 in 'Frontiers of Accelerator Technology', Ed S. I. Kurokawa, M. Month and S. Turner, pub World Scientific 1996.
- [8] H. Bruck, D. Gall et al, "Observation of periodic patterns in the persistent current fields of the superconducting HERA magnets", Proc IEEE Particle Accelerator Conference, San Francisco, 1991 pp. 2149.
- [9] H. Hemmes, M. J. Woudstra, H. J. ten Kate and J. Tenbrink, "Transport current dependence of the hysteresis loss in silver-sheathed BSCCO-2212 conductors", Cryogenics 34: 567-570 Suppl. ICEC 1994.
- [10] M.N. Wilson, G. Moritz, M. Anerella, G. Ganetis, A.K. Ghosh, W.V. Hassenzahl, A. Jain, P. Joshi, J. Kaugerts, C. Muehle, J. Muratore, R. Thomas, G. Walter, P. Wanderer, "Design Studies on Superconducting Cos θ Magnets for a Fast Pulsed Synchrotron", Proc MT-17, IEEE Trans. Applied Superconductivity Vol 12 No. 1 March 2002, p. 313.
- [11] M. Anerella, A.K. Ghosh, R. Soika, P. Wanderer, M.N. Wilson, W.V. Hassenzahl, J. Kaugerts, and G. Moritz, "Inter-strand Resistance Measurements in Cored Rutherford Cables", paper 5LG02 at this conference.
- [12] F. R. Fickett, "Oxygen free high conductivity copper at 4K: resistance and magnetoresistance", IEEE Trans MAG-19 No 3, pp228 (1983).

- [13] A.K. Ghosh, W.B. Sampson, E Gregory, T.S. Kreilick, "Anomalous low field magnetization in fine filament NbTi conductors", IEEE Trans MAG-23, No2, pp1724, (1987).
- [14] V. Arp, "Force flow single phase helium cooling systems", Adv Cryo. Eng. Vol 17 pp343 (1972).